AD NUMBER

ADB208950

NEW LIMITATION CHANGE

TO

Approved for public release, distribution unlimited

FROM

Distribution authorized to DoD only. Other requests shall be referred to Embassy of Australia, Head. Pub. Sec.-Def/Sci., 1601 Massachusetts Ave., NW, Washington, DC 20036.

AUTHORITY

DSTO ltr dtd 27 Aug 99

Modelling Time-of-Arrival Ambiguities in a Combined Acousto-optic and Crystal Video Receiver

Simon Rockliff

DEPARTMENT OF DEFENCE
DEFENCE SCIENCE AND TECHNOLOGY ORGANISATION

DISCLAIMER NOTICE

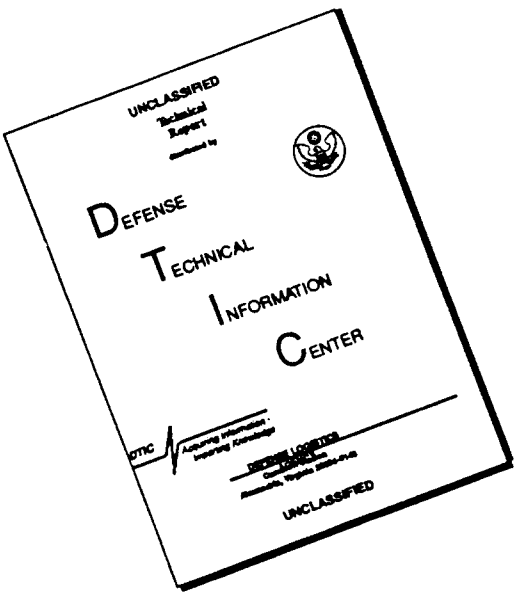

THIS DOCUMENT IS BEST QUALITY AVAILABLE. THE COPY FURNISHED TO DTIC CONTAINED A SIGNIFICANT NUMBER OF PAGES WHICH DO NOT REPRODUCE LEGIBLY.

Modelling Time-of-Arrival Ambiguities in a Combined Acousto-optic and Crystal Video Receiver

Simon Rockliff

Electronic Warfare Division
Electronics and Surveillance Research Laboratory

DSTO–RR–0062

ABSTRACT

The probability of received pulses overlapping in time is investigated for a combined acousto-optic/crystal video receiver. Theoretical analysis and computer simulation results are compared for a variety of high pulse density scenarios and for two crystal video band configurations. Upper and lower bounds are derived for the probability of pulse coincidence. It is shown that a small number of high duty cycle emitters in a frequency band will cause an unacceptable number of overlapped pulses in that bandwidth. The number of frequency subbands with crystal detectors which cover the acousto-optic receiver bandwidth is therefore a compromise between cost and complexity of implementation.

RELEASE LIMITATION

DEPARTMENT OF DEFENCE

DEFENCE SCIENCE AND TECHNOLOGY ORGANISATION

Published by

DSTO Electronics and Surveillance Research Laboratory

PO Box 1500
Salisbury, South Australia, Australia 5108

Telephone: (08) 259 5555
Facsimile: (08) 259 6567

AR No. 009-439

November 1995

Modelling time-of-arrival ambiguities in a combined acousto-optic and crystal video receiver

EXECUTIVE SUMMARY

This report investigates the probability of pulses overlapping in time being recorded in a combined acousto-optic/crystal video receiver for a variety of high pulse density scenarios. Overlapping pulses pose a problem of reconciliation of frequency reports from the AO receiver, and time of arrival and pulse width reports from the crystal video receiver. Subdividing the AO receiver bandwidth to cover it with a number of crystal video receivers is a method of decreasing the coincidence probability within a crystal video bandwidth, and avoiding further complicated processing later.

To evaluate the probability of pulses from a particular emitter overlapping in time with those from any other emitter, direct Monte Carlo simulation and theoretical approximations are compared. A Poisson approximation to the number of coincidences, based on the average pulse width and pulse repetition frequency, is derived. This approximation is accurate when considering a large number of low duty cycle emitters, and may be applied with care to higher duty cycle emitters. Upper and lower bounds are derived for the probability of coincidence between pulses from a particular emitter and those from any other emitter.

By taking the examples of 1 GHz bandwidth, and the same bandwidth subdivided into six subbands, it is shown that a small number of high duty cycle emitters together with some conventional emitters in a frequency band will cause numbers of overlapped pulses in that bandwidth which would be excessive for further real-time processing. As the number of frequency subbands increases, the number of signals occupying a band will in general decrease, thus decreasing the probability of coincidence. The number of crystal detector subbands required to cover the acousto-optic receiver bandwidth is therefore a compromise between cost and complexity of implementation. The results also have wider application for any wideband receivers such as crystal video or IFM receivers.

THIS PAGE IS INTENTIONALLY BLANK

Authors

Simon Rockliff
Electronic Warfare Division

Simon Rockliff has been with the Electronic Warfare Division of the DSTO since 1990, following the completion of his PhD. on the application of spread spectrum techniques to digital mobile radio. His current work involves the modelling and evaluation of Electronic Support Measures (ESM) and Radar Warning Receivers, and research into new techniques for receiving and identifying radar signals.

THIS PAGE IS INTENTIONALLY BLANK

Contents

Tables

1 Introduction

With the proliferation of high and medium pulse-repetition-frequency (PRF) airborne radars and instances of concentration of a large number of emitters in a small geographic area, such as the Malacca straits and near Singapore, high pulse density signal environments are likely to become more common. This has implications for the Australian Defence Force units which may have to operate in them, either in undertaking defence in Australia's area of direct military interest or as a consequence of peace-keeping missions. The in-band overlapping pulses which result from such environments cause problems for conventional wide open ESM receivers such as instantaneous frequency measurement (IFM) receivers and crystal video receivers.

The rationale for developing a channelised receiver is that the instantaneous bandwidth covered by the receiver is large, but the small channel bandwidths result in low noise floors, and hence increased sensitivity compared to IFM receivers. The channelisation allows the receiver to detect and measure frequencies of simultaneous pulses in high pulse density environments, and saturation of the receiver by a signal in one channel will have no effect on the ability of the receiver to simultaneously detect a signal in another channel at a sufficient frequency separation.

One channeliser implementation being developed at DSTO utilises acousto-optic (AO) technology. In this case the AO receiver covers an instantaneous bandwidth of 1.0 GHz by use of 108 consecutive channels each 9.25 MHz wide. This has advantages of light weight and low power but is unable to measure time-of-arrival (TOA) and pulse widths directly to a resolution sufficient for emitter identification by further processing. The time resolution of the AO channeliser is determined by the length of the integration period used (which may vary on application). Therefore parallel auxilliary sub-assemblies using crystal detectors are used to measure the TOA and pulse widths. This work investigates two proposals for the number of crystal detector subassemblies required in order to obtain reasonably unambiguous measurements for most circumstances. These were the use of a single crystal detector covering the whole 1 GHz bandwidth, and using 6 subband detectors, each covering 166.67 MHz, which matches the segmentation of the photodetector array during the data readout operation and is likely to have hardware implementation advantages over any other band division.

2 Methodology

The method used to assess the system performance with different numbers of crystal detectors was to examine the number of pulses which overlap within the nominated crystal detector bandwidths. Any pulses which overlap within a crystal detector bandwidth can cause an ambiguous reading, as it is assumed that the AO receiver will give two frequency readings, but only one TOA and PW measurement will be available from the crystal detector. This reading may be fully correct for one pulse (where it completely overlaps the other pulse), or may be a composite of the TOA for one pulse and the combined pulse width. In either case, unambiguous allocation of a pulse width or TOA reading to

a frequency report is impossible without further information being available. Attempting to correlate TOA and pulse width reports with frequency reports by using past history, can be a risky (and time-consuming) procedure when considering many modern emitters which can be agile in any of the parameters RF, pulse width and PRF. To meet processing time restrictions, it is far better to resolve ambiguities by measurement and avoid pushing the identification problem into the deinterleaving stage.

A figure must be chosen for an acceptable number of ambiguous pulses which can be tolerated by the further processing stages (ie. deinterleaving and clustering). After discussion with various researchers in the field, a value of 20% of pulses from any particular emitter was chosen as the limit of acceptability. This may be somewhat conservative for some proposed deinterleaving algorithms, but it is more in line with current implementations.

To investigate the capability of the receiver, a number of emitter environments must be specified, with the pulse densities considered being in excess of 100000 pulses per second at the receiver. In terms of Australia's perceived defence planning, the mix of emitters leading to this pulse density is likely to occur only in the 9–10 GHz band. This band includes a shipping navigation band and a substantial number of surface/low flyer search radars as well as missile threats and airborne pulse Doppler radars. Therefore the investigation centred on this band.

Either a theoretical or simulation approach may be used to examine the effect of the high pulse densities. Any theoretical approach relies on assumptions which may include a uniform frequency distribution over the band, or particular PRI and pulse width distributions. For this reason it was decided to directly simulate the incoming pulses, and compare the number of coincidences with that predicted from theory, given the same constraints as the simulation data. The emitters were made non-scanning, to achieve a reasonable pulse density with a restricted number of emitters. This can to some extent also be justified by the sensitivity of the receiver, which is sufficient to detect the sidelobes for any close radar. For a given pulse density, a larger number of scanning emitters would be required and would give results more akin to that predicted from random pulse distributions.

It is considered that the system should be able to deal with at most 2 simultaneous high pulse repetition frequency (HPRF) emitters for the following reasons:

- normal operation of airborne radar is generally in a HPRF/MPRF interlaced mode to obtain unambiguous velocity and range.
- a raster scan is usually employed, which together with the narrow beamwidths and moderate peak power, results in a smaller probability of being illuminated at a detectable power level.
- in the event of being constantly illuminated by 1 or 2 hostile HPRF or CW radars, it is likely that a target illumination mode for missile guidance is being used, and hence all other emitters can be ignored until the highest priority threat is dealt with. Any additional HPRF or CW emitters are likely to be recognized, and these in most cases will take precedence over other signals which may be obliterated.

A number of scenarios were designed to investigate the problem. Each scenario was run 20 times in each band with different random seeds to obtain different time offsets between pulse trains, and the average number of coincidences computed. The initial run assumed one time of arrival detector covering the whole 1 GHz band, and then the probability of coincidence in each of six 166.67 MHz subbands was examined.

The following scenarios were used:

1. 36 LPRF emitters in 9-10 GHz band, uniformly spaced in frequency
2. as for (1), plus 1 HPRF emitter
3. as for (1), plus 1 MPRF emitter
4. as for (1), plus 1 MPRF, 1HPRF emitters in same 166.67 MHz subband
5. as for (1), plus 2 HPRF emitters in same 166.67 MHz subband
6. as for (1), plus 2 MPRF emitters in same 166.67 MHz subband

A plot of emitter frequency, PRF and pulse width for the base scenario 1 is shown in Figure 1, and a table of the basic emitter parameters (ignoring jitters and PRI drifts used to randomise timing relationships for emitters with similar PRFs) is shown in Table 1.

3 Theoretical Prediction of Pulse Coincidence

Using Monte Carlo simulation to evaluate the probability of coincidence of pulse trains is very time consuming, and a theoretical result is preferable. Most of the literature on this subject deals with the statistics of multiple simultaneous window overlap, *eg* [1, 2, 3, 4, 5], where all window functions (corresponding to all pulse trains) must be simultaneously high for a pulse to be output. We are interested in the probability of any number of pulses from $(N-1)$ independent pulse trains interfering simultaneously with another independent pulse train. While it should be possible to use the results of [2] and [3] to derive the probability of coincidence on any one pulse train, a much simpler solution has been derived by Kazerman [6] for the case where all the pulse train PRIs are greater than all the pulse widths.

His solution can be extended to cover all cases very simply. Let pulse train i have a pulse repetition interval (PRI) T_i, and pulse width τ_i. We assume that the PRIs of the various pulse trains are mutually irrational or have very large lowest common multiples, and are started randomly phased with respect to one another. Then given that a pulse from pulse train 1 exists, the probability of no coincidence with a pulse from the kth pulse train can be written as

$$P(\text{no coincidence on 1 from } k) = \begin{cases} \frac{T_k-(\tau_k+\tau_1)}{T_k} & \tau_k+\tau_1 \le T_k \\ 0 & \tau_k+\tau_1 > T_k \end{cases} \quad (1)$$

Table 1: Basic parameters for emitters used in scenarios

Emitter	Frequency (MHz)	PRF	PW (μs)
1	9013.88	347.10	0.50
2	9046.66	726.74	1.00
3	9074.44	1104.97	0.80
4	9102.22	726.74	1.00
5	9130.0	1121.08	0.80
6	9157.78	2460.02	0.30
7	9185.56	809.72	1.05
8	9213.34	726.74	0.80
9	9241.12	719.94	0.63
10	9268.8	653.60	1.03
11	9296.68	735.29	0.12
12	9324.46	722.02	0.96
13	9352.24	780.03	0.54
14	9380.02	720.98	0.94
15	9407.8	500.00	0.99
16	9435.58	1440.92	0.46
17	9463.36	2127.66	0.28
18	9491.14	750.75	0.80
19	9518.92	1600.00	0.30
20	9546.7	750.75	0.70
21	9574.48	1011.12	5.04
22	9602.26	1636.66	0.98
23	9630.04	900.09	0.80
24	9657.82	998.00	0.62
25	9685.6	1470.59	0.50
26	9713.38	1683.50	0.60
27	9741.16	841.75	0.70
28	9768.94	809.06	0.90
29	9796.72	999.70	0.50
30	9824.5	1010.71	0.20
31	9852.28	1100.35	0.17
32	9880.06	969.93	3.00
33	9907.84	827.82	1.00
34	9935.62	1680.11	0.25
35	9963.4	2032.93	0.15
36	9991.18	2449.78	0.50
MPRF 1	9580.0	10000.00	13.00
MPRF 2	9533.0	15220.70	13.00
HPRF 1	9580.0	130005.00	1.60
HPRF 2	9533.0	166003.00	1.80

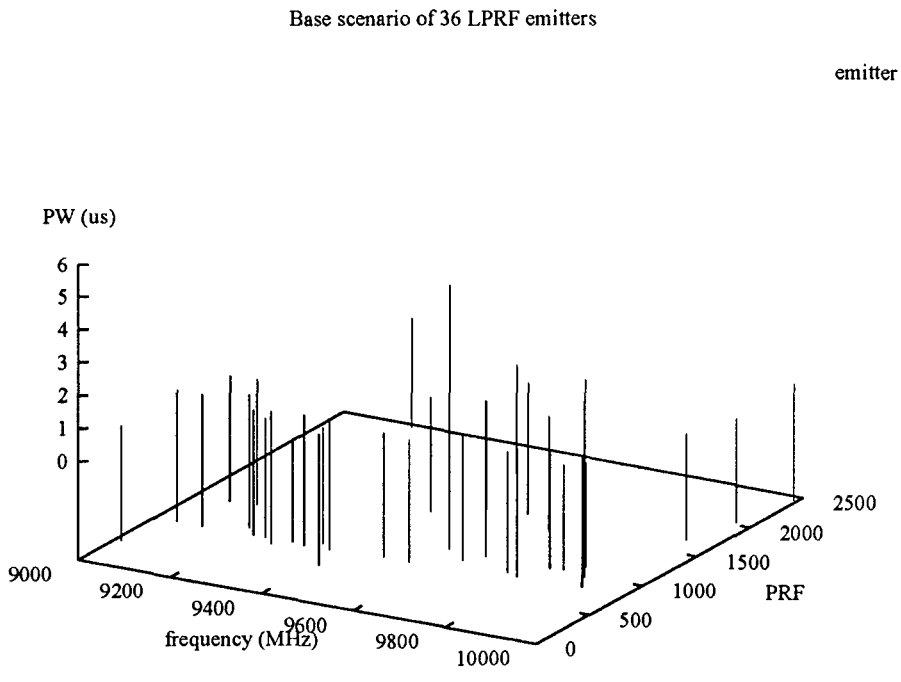

Figure 1: Emitter frequency, PRF, and pulse width for 36 naval type emitters distributed uniformly in frequency over a 1 GHz bandwidth.

and as the pulse trains are independent, the probability that at least one pulse from any pulse train coincides with the pulse from train 1 is

$$P(\text{coincidence on 1 from any other train}) = \begin{cases} 1 - \prod_{k=2}^{N} \left(1 - \frac{(\tau_k + \tau_1)}{T_k}\right) & \text{if } \tau_k + \tau_1 \leq T_k \ \forall k \\ 1 & \text{otherwise} \end{cases} \tag{2}$$

An alternative approach to the problem is to assume the sum of N regular pulse trains (subject to the above assumptions) has an interarrival time given by the exponential distribution. If the pulse widths are small compared with the period for all emitters, the correct interarrival time distribution asymptotically approaches the exponential distribution with increasing N. The proof for this approach is given in [7]. The average pulse width $\bar{\tau}$ of all the interfering emitters $(2 \ldots N)$ and the sum of their PRFs may be calculated as

$$\bar{\tau} = \frac{\sum_{k=2}^{N} \tau_k / T_k}{\sum_{k=2}^{N} 1/T_k} \tag{3}$$

and

$$\sum_{k=2}^{N} \mathrm{prf}_k = \sum_{k=2}^{N} 1/T_k \tag{4}$$

respectively.

An overlap on a pulse from emitter 1 is assumed to occur if a pulse arrives within the pulse width of emitter 1 or if one had previously arrived within the average pulse width of all the other pulses. From the theory of Poisson arrivals [8], the probability of a coincidence occuring may be computed simply as

$$\begin{aligned} P(\text{coincidence on 1}) &= 1 - P(\text{no arrivals in time } (\tau_1 + \bar{\tau})) \\ &= 1 - \exp\left[-(\tau_1 + \bar{\tau})\left(\sum_{k=2}^{N} \mathrm{prf}_k\right)\right] \end{aligned} \tag{5}$$

This enables the probability of coincidence on a new emitter being introduced into an existing environment to be expressed as a function of the current average pulse width and total received pulse density. It is shown in Appendix A that Equation 5 forms a lower bound to the probability of coincidence.

The above formulae were used to predict the rate of coincidence for each of the simulated pulse trains, and the results compared to those produced by the simulation.

4 Results

Tabulated results for each of the cases considered are given in Appendix B. The results indicate that for the 36 maritime type emitters in a 1 GHz band, the rate of coincidence on any one emitter is generally in the range 3–7% of the transmitted pulses. The exception is the longer pulses (3μs and 5μs, whereas the average pulse width is 0.7μs), where the rates of coincidence were approximately 13% and 20% respectively. These correspond to the emitters with the highest duty cycle (0.0029 and 0.005 *cf* less than 0.001 for all other emitters). For this scenario, the two theoretical approaches gave almost identical results and were a close match to the simulation results.

When a medium PRF (MPRF) emitter, with pulse width 13μs and PRF 10000 pulses per second, is introduced into the scenario, a substantial rise in the number of pulse coincidences is noted. The minimum coincidence rate is about 16%, the maximum 34% and the median rate is about 18% over all the LPRF emitters. The MPRF emitter itself suffers a coincidence rate of 42.5%. The lowest pulse coincidence rates would be marginally acceptable for further processing, with the others totally unacceptable. These results are predicted by the formula of Kazerman to within 1% point of the simulation figure. The Poisson approximation is somewhat more inaccurate, usually being slightly lower than the simulation value.

If a high PRF (HPRF) emitter, with pulse width 1.7μs and PRF of 166000 pulses per second, is used instead of the MPRF emitter, the probability of coincidence for all the low PRF emitters rises yet again, with rates beginning at 35% and one emitter recording

a coincidence on every pulse. These rates would clearly cause problems for any further processing. The HPRF emitter itself recorded a pulse coincidence rate of 9.65%, which should be sufficiently low to be able to identify this emitter. In this case, Kazerman's formula gave very good results for the rate of pulse coincidence. On the other hand, the values predicted by the Poisson arrivals model were invariably low by several percentage points, with the exception of the prediction for the HPRF emitter, which closely matched the simulation result and Kazerman' formula. It would appear that the Poisson arrival formula breaks down when an emitter with a high duty cycle (*eg* 0.3) is introduced, and hence should be used with caution for these cases.

As can be expected, the introduction of one HPRF and one MPRF emitter, or 2 MPRF or 2 HPRF emitters into the basic scenario of 36 maritime type emitters leads to still higher rates of coincidence for all emitters, at levels impractical for further processing. These cases continue to demonstrate the accuracy of Kazermans formula in predicting the frequency of coincidence, and confirm the trend of the Poisson arrival formula to give low estimates of pulse coincidence for these cases.

The simulations were then repeated with the 1 GHz band divided into 6 subbands, each 166.67 MHz wide. Assuming the uniform frequency distribution used in the previous scenarios for the low PRF emitters, the simulation results (for no HPRF or MPRF emitters) were then calculated for each of the subbands. The probability of coincidence was reduced roughly by a factor of 6–10, as expected from the bandwidth reduction. In all cases the two prediction methods gave identical results. The match with the simulation results was reasonably close, and although the error as a proportion of the coincidence rate was higher, the absolute error in the coincidence rate stayed about the same. This is due in part to the small number of pulse coincidences in the sample leading to a "granularity" in the measurements, and any effects of synchronism between pulse trains having more effect at these low coincidence levels.

Introduction of a MPRF emitter into the scenario affects only that subband in which that emitter is located. A MPRF emitter resulted in coincidence rates of 14–20% for the LPRF emitters (median value 14.5%), and the MPRF emitter having a rate of 9.76%. Both prediction formulae were relatively close, although typically the Poisson arrivals formula was fractionally low. The HPRF emitter resulted in unacceptable clash rates of 35% to 100% (median 42%) for the 6 LPRF emitters, with the HPRF emitter having only 2% of pulses corrupted.

Predictably, the system recorded unacceptable pulse coincidence levels ($\geq$ 30%) with more than 1 MPRF or 1 HPRF emitter (assuming they both have high duty cycles as typically found in airborne radars) simultaneously with the 6 LPRF emitters. However, the effect is limited to one subband, as all other subbands function independently.

The use of the Poisson formula is limited by the reservations mentioned previously. However, it is useful to get an idea of the probability of coincidence. To this end, three surfaces are plotted in Figures 2–4 showing the probability of coincidence as a function of PRF and varying pulse width, for a fixed pulse width (either the average pulse width or the specific emitter pulse width) of 0.5,2.0 or 10.0 μs. Contours of constant probability of coincidence are projected onto the (PRF, pulse width) plane.

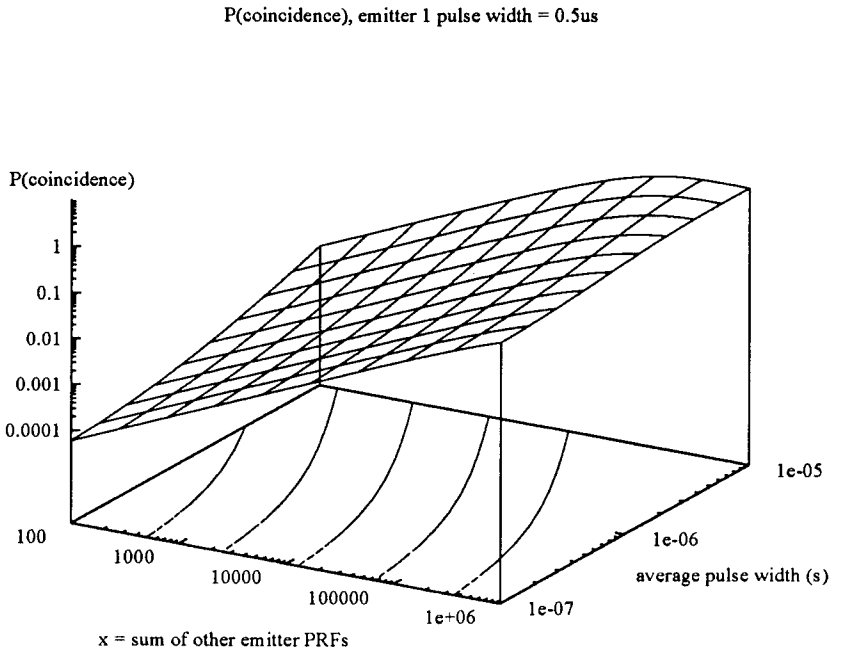

Figure 2: P(Coincidence on emitter #1) vs sum of other emitter PRFs, $\tau_1 = 0.5\mu s$

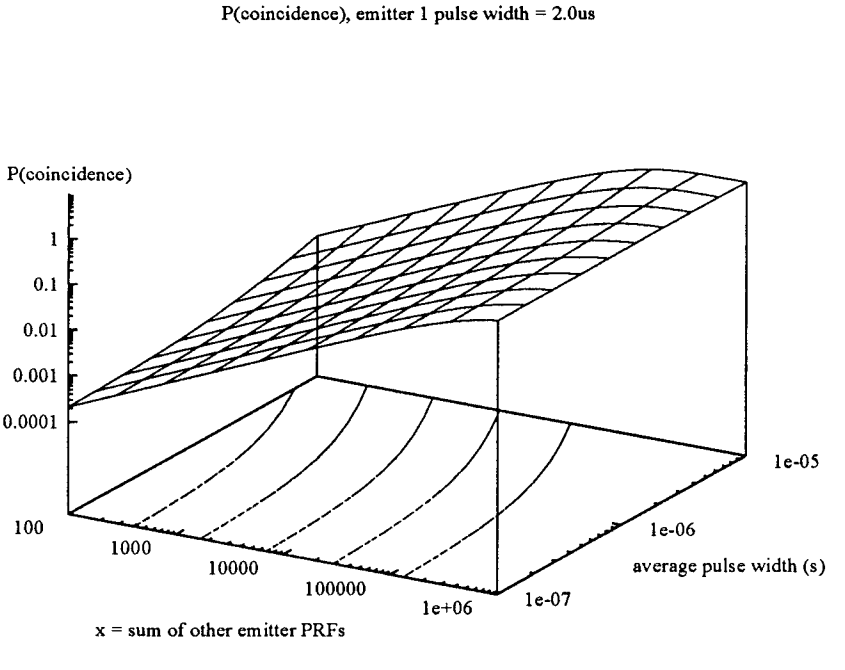

Figure 3: P(Coincidence on emitter #1) vs sum of other emitter PRFs, $\tau_1 = 2\mu s$

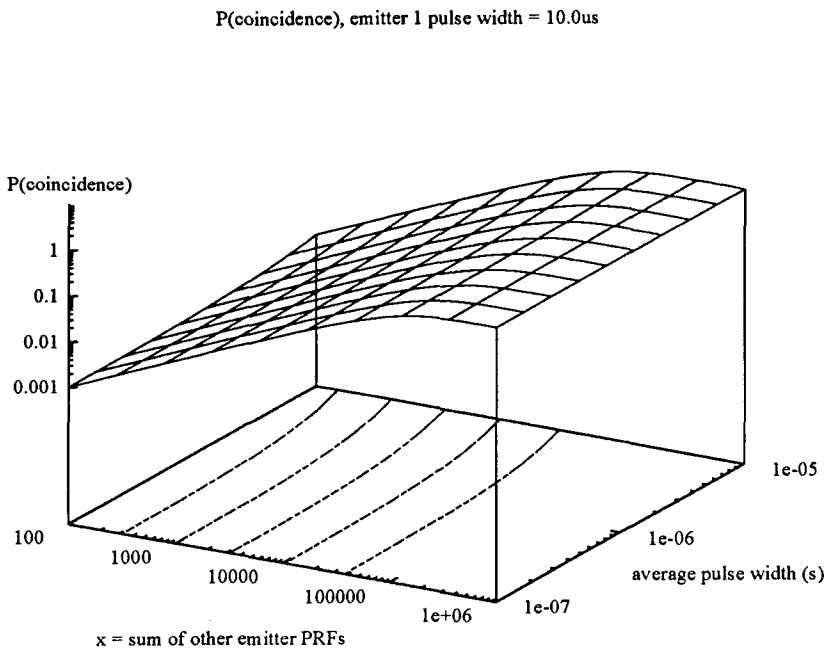

Figure 4: P(Coincidence on emitter #1) vs the sum of other emitter PRFs, $\tau_1 = 10\mu s$

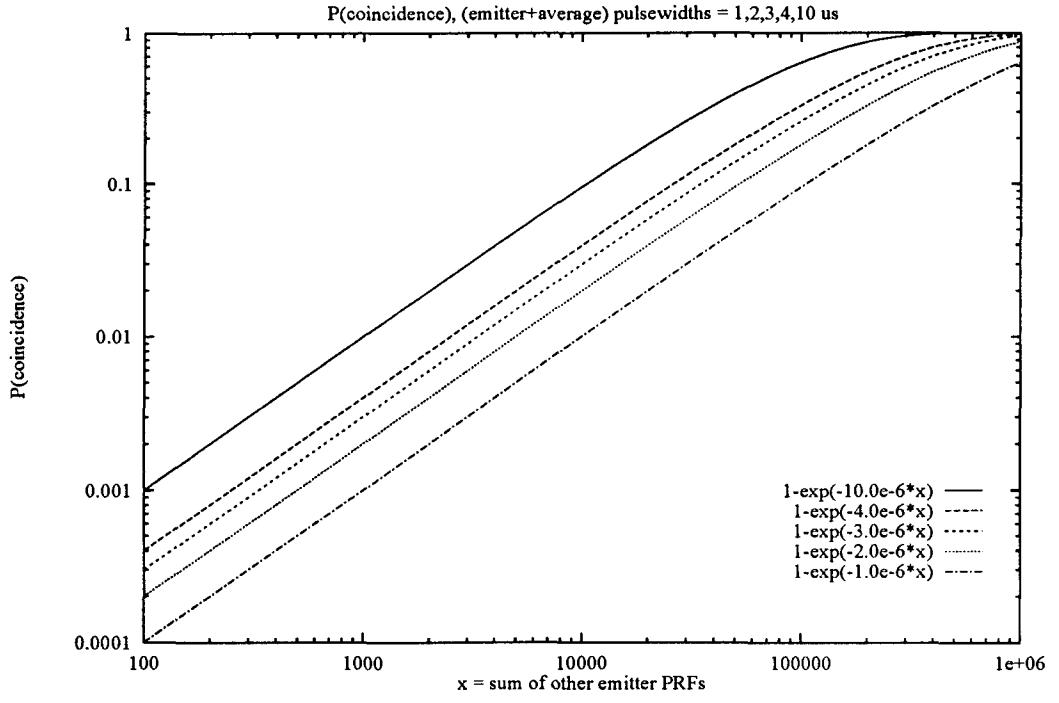

Figure 5: P(Coincidence on emitter #1) vs sum of other emitter PRFs, for $(\tau_1 + \bar{\tau}) = 1, 2, 3, 4, 10\mu s$

These graphs show the relationship between the duty cycle and the probability of coincidence. The introduction of a MPRF emitter with long pulse lengths or a higher duty cycle HPRF emitter moves the operating point on the surface up the gradient to a higher probability of coincidence. Any increase in PRF for a given pulse width, or increase in pulse width for a given PRF, will increase the probability of coincidence. The results formalize an intuitively correct result.

Figure 5 shows the coincidence probability of an emitter (taken as emitter 1) versus the sum of the other emitter PRFs for the combined pulse width of {emitter 1 + average pulse width over all other emitters}. For the region below $P(\text{coincidence}) = 0.1$, the curves are linear and the approximation to the correct formula of Kazerman is good. In fact, it can be shown (see Appendix A) that the probability of coincidence is upperbounded by the straight line

$$P(\text{coincidence on 1}) = \left(\sum_{k=2}^{N} \text{prf}_k\right)(\tau_1 + \bar{\tau}) \tag{6}$$

which is a close upper bound for scenarios with low duty cycle emitters and low pulse densities.

5 Summary

The results of the simulation of pulse coincidence and the theoretical results of Kazerman agree closely for all scenarios investigated. An alternative approach to coincidence prediction based on Poisson arrivals at the overall PRF rate, was a close approximation where the duty cycle of the emitters was small but led to low estimates when one or more high duty cycle emitters were introduced. Bounds may be computed on the probability of pulse coincidence based on the measureable quantities of average PRF and average pulse width.

The results clearly demonstrate the catastrophic effect of high duty cycle emitters on the ability of a broadband crystal detector to make unambiguous time of arrival and pulse width measurements in environments of even comparatively low pulse density. If a single 1 GHz bandwidth is used, the introduction of a single tracking HPRF or MPRF emitter such as that found in airborne pulse Doppler radars will cause the coincidence rate for all other emitters to become unacceptable or only marginally acceptable for the further processing and data fusion with frequency information from an AO receiver.

By subdividing the band to six subbands, the effect of the high duty cycle emitter is constrained to one subband. It has been shown that for as few as six other emitters simultaneously active in the subband, the probability of coincidence is still likely to be too high to be acceptable for the period of time that the high duty cycle emitter is illuminating the receiver. However, it must be remembered that the situation considered here is a worst case, in that the HPRF or MPRF emitter (and indeed most other emitters) will normally be scanning and not present for most of the time. Due to cost and complexity considerations, it does not seem practical or desirable to further subdivide the band.

These results apply to any type of receiver using an instantaneous wide bandwidth and indicate the necessity of channelisation in any sensitive receiver likely to operate in areas of high pulse density. They also enable the percentage of pulses from a specific emitter which overlap any of those from other emitters to be estimated from average pulse density and average pulse width measurements. This is useful in calculating the estimated proportion of corrupted pulses in a real environment for any crystal video receiver.

References

1. B.R. Hatcher. Intercept probability and intercept time. *Electronic Warfare and Defence Electronics*, pages 95–103, March 1976.

2. A.G. Self and B.G Smith. Intercept time and its prediction. *IEE Proceedings Part F*, 132(4):215–222, July 1985.

3. K.S. Miller and R.J. Schwarz. On the interference of pulse trains. *Journal of Applied Physics*, 24(8):1032–1036, August 1953.

4. S. Stein and D. Johansen. A statistical description of coincidences among random pulse trains. *Proceedings of the IRE*, 46:827–830, 1958.

5. George T. Demos and Mark S. Weprin. Probability of pulse coincidence in a multiple radar environment. *IEEE Transactions on Aerospace and Electronic Systems*, AES-19(4):635–640, 1983.

6. Philip Kazerman. Frequency of pulse coincidence given n radars of different pulse widths and PRFs. *IEEE Transactions on Aerospace and Electronic Systems*, AES-7:1013–1014, 1971.

7. D.R. Cox and W.L. Smith. The superposition of several strictly periodic sequences of events. *Biometrika*, 40 Parts 1 and 2:1–11, 1953.

8. Athanasios Papoulis. *Probability, Random Variables and Stochastic Processes*, chapter 3. McGraw-Hill International, second edition, 1984.

Appendix A
Derivation of Bounds on Coincidence Probability

It is straightforward to derive an upper and lower bound for the probability of a pulse from emitter 1 coinciding with a pulse from any other emitter.

We have

$$P(\text{coincidence on 1 from any other train}) = \begin{cases} 1 - \prod_{k=2}^{N}\left(1 - \frac{(\tau_k+\tau_1)}{T_k}\right) & \text{if } \tau_k + \tau_1 \le T_k \ \forall k \\ 1 & \text{otherwise} \end{cases} \tag{A1}$$

Consider the case where

$$\tau_k + \tau_1 \le T_j \qquad \forall j,k$$

We hypothesise that

$$P(\text{coincidence on 1 from any other train}) \le \tilde{P} = \left(\sum_{j=2}^{N} \text{prf}\right)(\bar{\tau} + \tau_1) \tag{A2}$$

so that $\tilde{P}$ is an upper bound to Equation A1, where

$$\begin{aligned} \bar{\tau} &= \text{average pulse width over emitters 2 to N} \\ &= \frac{\sum_{k=2}^{N}(\tau_k/T_k)}{\sum_{k=2}^{N}(1/T_k)} \end{aligned} \tag{A3}$$

For the case where $N = 2$ it is obviously true:

$$\begin{aligned} P(\text{coincidence on 1 from emitter 2}) = P_2 &= 1 - \left(1 - \left(\frac{1}{T_2}\right)(\tau_2 + \tau_1)\right) \\ &= (\text{prf}_2)(\tau_2 + \tau_1) \end{aligned}$$

For $N = 3$

$$\begin{aligned} P(\text{coincidence on 1 from 2 or 3}) = P_3 &= 1 - \left(1 - \frac{(\tau_2+\tau_1)}{T_2}\right)\left(1 - \frac{(\tau_3+\tau_1)}{T_3}\right) \\ &= \frac{\tau_2+\tau_1}{T_2} + \frac{\tau_3+\tau_1}{T_3} - \left(\frac{\tau_2+\tau_1}{T_2}\right)\left(\frac{\tau_3+\tau_1}{T_3}\right) \\ &\le \frac{\tau_2+\tau_1}{T_2} + \frac{\tau_3+\tau_1}{T_3} \\ &= \left(\frac{1}{T_2} + \frac{1}{T_3}\right)\left[\frac{\left(\frac{\tau_2}{T_2} + \frac{\tau_3}{T_3}\right)}{\left(\frac{1}{T_2} + \frac{1}{T_3}\right)} + \tau_1\right] \\ &= \left(\sum_{k=2}^{3} \text{prf}_k\right)[\bar{\tau} + \tau_1] \end{aligned}$$

and hence is true for $N = 3$.

Now consider the case of P_n, and let

$$X_n = \sum_{k=2}^{n} \frac{\tau_k + \tau_1}{T_k}$$

Then we assume

$$\begin{aligned} P_{n-1} &= 1 - (1 - (X_{n-1} - X'_{n-1})) \\ &= X_{n-1} - X'_{n-1} \end{aligned}$$

is true, where X'_{n-1} is the remainder term. P_n is defined as

$$\begin{aligned} P_n &= 1 - (1 - X_{n-1} + X'_{n-1})(1 - (\tau_n + \tau_1)/T_n) \\ &= X_{n-1} - X'_{n-1} + \frac{\tau_n + \tau_1}{T_n} - \left(\frac{\tau_n - \tau 1}{T_n}\right)(X_{n-1} - X'_{n-1}) \\ &= \left(X_{n-1} + \frac{\tau_n + \tau_1}{T_1}\right) - \left(X'_{n-1} + \left(\frac{\tau_n + \tau_1}{T_n}\right) P_{n-1}\right) \\ &= X_n - X'_n \end{aligned}$$

It follows simply then that

$$\begin{aligned} X_{n-1} &> X'_{n-1} \\ X_{n-1} + \frac{\tau_n + \tau_1}{T_n} &> X'_{n-1} + \frac{\tau_n + \tau_1}{T_n} \\ &> X'_{n-1} + \left(\frac{\tau_n + \tau_1}{T_n}\right) P_{n-1} \\ X_n &> X'_n \end{aligned}$$

Hence as P_2 and P_3 are true and $P_{n-1} \Rightarrow P_n$, the upper bound, Equation A2 is proved by induction.

The lower bound can be shown to be given by Equation 5 derived from the Poisson approximation.

Consider

$$P(\text{no coincidence}) = \prod_{k=2}^{N} \left(1 - \frac{\tau_k + \tau_1}{T_k}\right) \tag{A4}$$

$$\log P(\text{no coincidence}) = \sum_{k=2}^{N} \log \left(1 - \frac{\tau_k + \tau_1}{T_k}\right) \tag{A5}$$

$$\tag{A6}$$

Now

$$\log(1 - z) = -z - \frac{z^2}{2!} - \frac{z^3}{3!} - \frac{z^4}{4!} - \ldots \qquad \forall > 0, z < 1$$

hence

$$\begin{aligned}
\log P(\text{no coincidence}) &= \sum_{k=2}^{N}\left(-\frac{\tau_k+\tau_1}{T_k}-\frac{1}{2!}\left(\frac{\tau_k+\tau_1}{T_k}\right)^2-\frac{1}{3!}\left(\frac{\tau_k+\tau_1}{T_k}\right)^3-\frac{1}{4!}\left(\frac{\tau_k+\tau_1}{T_k}\right)^4-\ldots\right)\\
P(\text{no coincidence}) &= \exp\left[-\sum_{k=2}^{N}\left(\frac{\tau_k+\tau_1}{T_k}+\frac{1}{2!}\left(\frac{\tau_k+\tau_1}{T_k}\right)^2+\frac{1}{3!}\left(\frac{\tau_k+\tau_1}{T_k}\right)^3+\ldots\right)\right]\\
&< \exp\left[-\left(\sum_{k=2}^{N}\frac{\tau_k+\tau_1}{T_k}\right)\right]\\
&= \exp\left[-\left(\frac{\sum_{k=2}^{N}\tau_k/T_k}{\sum_{k=2}^{N}1/T_k}+\tau_1\right)\left(\sum_{k=2}^{N}1/T_k\right)\right]\\
&= \exp\left[-(\bar{\tau}+\tau_1)\left(\sum_{k=2}^{N}\text{prf}_k\right)\right]
\end{aligned}$$

Hence a lower bound for the probability of coincidence of a pulse from emitter 1 with a pulse from any other emitter is obviously

$$P(\text{coincidence on 1 from any other emitter}) = 1-\exp\left[-(\bar{\tau}+\tau_1)\left(\sum_{k=2}^{N}\text{prf}_k\right)\right] \qquad (A7)$$

which is simply Equation 5.

Appendix B
Tables of Simulated and Predicted Results

The following tables compare the predicted coincidence rates with those obtained from simulation. The emitter numbers refer to those defined previously in Table 1.

The first group of tables covers the coincidence rates of the 36 low PRF emitters in the full 1 GHz bandwidth, with up to 2 MPRF or 2 HPRF emitters also present in the band.

The next group of tables covers the same scenarios, but where only a 166.67 MHz subband of the 1 GHz bandwidth is considered, which contains 6 LPRF emitters.

To compare with the subband already examined, rates are given for the other subbands in the 1 GHz bandwidth. The HPRF and MPRF emitters are not present in these subands.

To ascertain at what number of emitters in a subband the MPRF and HPRF emitters start to cause unacceptable pulse coincidences, emitters are introduced gradually into the subband and the effect of adding a MPRF or HPRF emitter observed.

Table B1: Results for 36 low PRF emitters, 1 GHz bandwidth

	Simulation Results			Predicted percentage	
emitter	pulses recvd	clashes	percentage	Poisson	Kazerman
1	4167	173	4.15	4.81	4.81
2	2907	171	5.88	6.58	6.59
3	4420	221	5.00	5.81	5.81
4	2907	177	6.09	6.58	6.59
5	4480	288	6.43	5.80	5.81
6	9839	370	3.76	3.93	3.94
7	3240	206	6.36	6.75	6.76
8	2907	172	5.92	5.86	5.87
9	2880	137	4.76	5.25	5.25
10	2614	172	6.58	6.71	6.71
11	2941	112	3.81	3.37	3.37
12	2888	182	6.30	6.44	6.45
13	3120	141	4.52	4.91	4.92
14	2884	195	6.76	6.37	6.38
15	2000	127	6.35	6.59	6.60
16	5764	256	4.44	4.56	4.56
17	8508	304	3.57	3.88	3.89
18	3002	183	6.10	5.86	5.87
19	6398	255	3.99	3.98	3.99
20	3005	157	5.22	5.50	5.50
21	4043	767	18.97	19.81	19.88
22	6546	394	6.02	6.35	6.35
23	3600	201	5.58	5.84	5.84
24	3992	202	5.06	5.18	5.18
25	5882	258	4.39	4.70	4.70
26	6733	342	5.08	5.03	5.03
27	3374	181	5.36	5.48	5.49
28	3237	170	5.25	6.21	6.22
29	3998	212	5.30	4.74	4.75
30	4042	138	3.41	3.65	3.66
31	4402	142	3.23	3.54	3.54
32	3880	499	12.86	13.38	13.41
33	3311	207	6.25	6.57	6.57
34	6719	271	4.03	3.80	3.81
35	8138	274	3.37	3.44	3.44
36	9796	442	4.51	4.61	4.61

Table B2: Results: 36 low PRF emitters and 1 MPRF emitter, 1 GHz bandwidth

	Simulation Results			Predicted percentage	
emitter	pulses recvd	clashes	percentage	Poisson	Kazerman
1	1389	234	16.85	16.83	17.66
2	2904	581	20.01	18.79	19.67
3	4420	763	17.26	17.95	18.81
4	2902	567	19.54	18.79	19.67
5	4480	831	18.55	17.95	18.81
6	9839	1635	16.62	15.90	16.71
7	3240	635	19.60	18.97	19.86
8	2902	557	19.19	18.00	18.86
9	2880	523	18.16	17.32	18.17
10	2609	525	20.12	18.92	19.80
11	2934	455	15.51	15.25	16.05
12	2884	550	19.07	18.63	19.51
13	3120	543	17.40	16.95	17.79
14	2880	589	20.45	18.55	19.43
15	2000	410	20.50	18.79	19.67
16	5763	999	17.33	16.58	17.41
17	8465	1401	16.55	15.84	16.65
18	3003	589	19.61	17.99	18.86
19	6398	1176	18.38	15.94	16.76
20	3005	546	18.17	17.60	18.45
21	4043	1374	33.98	33.05	34.33
22	6546	1262	19.28	18.56	19.45
23	3601	699	19.41	17.97	18.84
24	3992	719	18.01	17.25	18.10
25	5882	878	14.93	16.73	17.57
26	6733	1181	17.54	17.10	17.95
27	3374	613	18.17	17.59	18.44
28	3237	599	18.50	18.38	19.25
29	3999	691	17.28	16.77	17.61
30	4043	653	16.15	15.57	16.37
31	4402	707	16.06	15.44	16.25
32	3880	1066	27.47	26.19	27.27
33	3311	581	17.55	18.77	19.65
34	6720	1122	16.70	15.74	16.55
35	8138	1320	16.22	15.34	16.14
36	9798	1697	17.32	16.65	17.49
37	39995	16862	42.16	42.24	42.54

Table B3: Results: 36 low PRF and 1 HPRF emitters, 1 GHz bandwidth

	Simulation Results			Predicted percentage	
emitter	pulses recvd	clashes	percentage	Poisson	Kazerman
1	1389	558	40.17	35.02	41.15
2	2904	1456	50.14	41.31	50.01
3	4420	2019	45.68	38.82	46.46
4	2902	1443	49.72	41.31	50.01
5	4480	2065	46.09	38.82	46.46
6	9841	3716	37.76	32.21	37.43
7	3240	1655	51.08	41.90	50.87
8	2902	1315	45.31	38.86	46.50
9	2880	1253	43.51	36.70	43.47
10	2609	1297	49.71	41.68	50.54
11	2934	965	32.89	29.74	34.17
12	2885	1423	49.32	40.83	49.31
13	3120	1296	41.54	35.52	41.85
14	2880	1420	49.31	40.59	48.96
15	2000	1015	50.75	41.22	49.86
16	5764	2316	40.18	34.42	40.37
17	8465	3165	37.39	31.95	37.07
18	3003	1400	46.62	38.86	46.49
19	6400	2386	37.28	32.24	37.46
20	3005	1308	43.53	37.60	44.72
21	4043	4043	100.00	74.24	100.00
22	6548	3246	49.57	40.97	49.57
23	3601	1665	46.24	38.84	46.48
24	3992	1713	42.91	36.55	43.27
25	5882	2415	41.06	34.94	41.09
26	6734	2867	42.57	36.24	42.87
27	3374	1505	44.61	37.59	44.71
28	3237	1528	47.20	40.09	48.25
29	3999	1637	40.94	34.98	41.12
30	4043	1423	35.20	30.87	35.64
31	4402	1530	34.76	30.45	35.09
32	3880	3192	82.27	60.96	82.41
33	3312	1646	49.70	41.30	50.00
34	6721	2460	36.60	31.55	36.54
35	8138	2801	34.42	30.14	34.70
36	9799	4000	40.82	34.88	41.03
37	663995	64081	9.65	9.65	9.67

Table B4: Results: 36 low PRF and 2 MPRF emitters, 1 GHz bandwidth

	Simulation Results			Predicted percentage	
emitter	pulses recvd	clashes	percentage	Poisson	Kazerman
1	1389	475	34.20	32.28	34.58
2	2904	1076	37.05	34.37	36.79
3	4420	1534	34.71	33.49	35.86
4	2902	1073	36.97	34.37	36.79
5	4480	1606	35.85	33.49	35.86
6	9842	3300	33.53	31.31	33.57
7	3240	1192	36.79	34.57	37.00
8	2902	1063	36.63	33.53	35.90
9	2880	1021	35.45	32.81	35.14
10	2609	973	37.29	34.51	36.93
11	2934	942	32.11	30.59	32.81
12	2884	1043	36.17	34.21	36.61
13	3120	1072	34.36	32.42	34.73
14	2880	1075	37.33	34.12	36.52
15	2000	747	37.35	34.36	36.77
16	5763	1961	34.03	32.03	34.33
17	8465	2837	33.51	31.24	33.50
18	3003	1095	36.46	33.53	35.90
19	6398	2224	34.76	31.35	33.61
20	3005	1059	35.24	33.11	35.45
21	4043	2107	52.11	49.12	52.36
22	6546	2388	36.48	34.17	36.59
23	3600	1295	35.97	33.51	35.88
24	3992	1392	34.87	32.74	35.08
25	5882	1885	32.05	32.20	34.51
26	6734	2307	34.26	32.60	34.93
27	3374	1194	35.39	33.10	35.45
28	3237	1157	35.74	33.95	36.34
29	3999	1372	34.31	32.23	34.54
30	4043	1329	32.87	30.93	33.17
31	4402	1453	33.01	30.80	33.04
32	3880	1723	44.41	42.14	44.98
33	3311	1167	35.25	34.36	36.77
34	6720	2252	33.51	31.13	33.38
35	8138	2668	32.78	30.70	32.92
36	9797	3372	34.42	32.13	34.44
37	39999	26036	65.09	61.12	65.28
38	60876	34936	57.39	55.47	57.48

Table B5: Results: 36 low PRF, 1 MPRF and 1HPRF emitters, 1 GHz bandwidth

	Simulation Results			Predicted percentage	
emitter	pulses recvd	clashes	percentage	Poisson	Kazerman
1	1389	674	48.52	43.22	49.10
2	2904	1667	57.40	48.98	57.01
3	4420	2345	53.05	46.71	53.85
4	2902	1683	57.99	48.98	57.01
5	4480	2390	53.35	46.71	53.85
6	9842	4521	45.94	40.65	45.75
7	3240	1842	56.85	49.51	57.77
8	2902	1599	55.10	46.74	53.88
9	2880	1480	51.39	44.76	51.18
10	2609	1520	58.26	49.31	57.48
11	2934	1280	43.63	38.38	42.80
12	2884	1632	56.59	48.54	56.39
13	3120	1561	50.03	43.68	49.72
14	2880	1627	56.49	48.32	56.08
15	2000	1127	56.35	48.89	56.87
16	5765	2776	48.15	42.68	48.39
17	8465	3859	45.59	40.41	45.43
18	3003	1614	53.75	46.74	53.88
19	6400	2980	46.56	40.68	45.78
20	3005	1570	52.25	45.59	52.29
21	4043	4043	100.00	78.49	100.00
22	6548	3695	56.43	48.67	56.62
23	3600	1952	54.22	46.73	53.87
24	3992	2010	50.35	44.63	51.00
25	5882	2782	47.30	43.16	49.04
26	6734	3390	50.34	44.34	50.64
27	3374	1775	52.61	45.58	52.29
28	3237	1772	54.74	47.86	55.44
29	3999	1936	48.41	43.19	49.07
30	4043	1773	43.85	39.42	44.14
31	4402	1922	43.66	39.03	43.64
32	3880	3313	85.39	66.73	85.22
33	3312	1859	56.13	48.97	57.00
34	6721	3035	45.16	40.04	44.95
35	8138	3523	43.29	38.75	43.29
36	9799	4776	48.74	43.10	48.99
37	40000	39999	100.00	95.05	100.00
38	663993	153023	23.05	22.08	23.04

Table B6: Results: 36 low PRF emitters, 2 HPRF emitters, 1 GHz bandwidth

	Simulation Results			Predicted percentage	
emitter	pulses recvd	clashes	percentage	Poisson	Kazerman
1	1389	795	57.24	50.54	57.22
2	2904	1888	65.01	58.14	66.91
3	4420	2766	62.58	55.22	63.17
4	2902	1944	66.99	58.14	66.91
5	4480	2821	62.97	55.22	63.17
6	9842	5219	53.03	47.05	52.88
7	3240	2164	66.79	58.83	67.80
8	2902	1856	63.96	55.25	63.19
9	2880	1733	60.17	52.63	59.86
10	2609	1763	67.57	58.57	67.45
11	2934	1453	49.52	43.82	48.89
12	2885	1917	66.45	57.58	66.18
13	3120	1835	58.81	51.18	58.03
14	2880	1889	65.59	57.30	65.81
15	2000	1351	67.55	58.02	66.74
16	5765	3229	56.01	49.82	56.34
17	8465	4451	52.58	46.70	52.45
18	3003	1880	62.60	55.25	63.19
19	6400	3379	52.80	47.07	52.91
20	3005	1824	60.70	53.72	61.25
21	4043	4043	100.00	89.13	100.00
22	6548	4339	66.26	57.79	66.48
23	3600	2282	63.39	55.24	63.18
24	3992	2348	58.82	52.45	59.64
25	5882	3336	56.72	50.49	57.17
26	6734	3953	58.70	52.10	59.21
27	3374	2065	61.20	53.72	61.24
28	3237	2069	63.92	56.71	65.07
29	3999	2266	56.66	50.51	57.19
30	4043	2028	50.16	45.30	50.70
31	4402	2195	49.86	44.74	50.02
32	3880	3614	93.14	78.53	92.93
33	3312	2205	66.58	58.14	66.90
34	6721	3475	51.70	46.18	51.80
35	8138	4018	49.37	44.36	49.56
36	9799	5591	57.06	50.44	57.13
37	520014	312774	60.15	48.21	60.34
38	664000	328404	49.46	41.93	49.60

Table B7: Results for 6 low PRF emitters, 166.67 MHz bandwidth

	Simulation Results			Predicted percentage	
emitter	pulses recvd	clashes	percentage	Poisson	Kazerman
19	6398	62	0.97	1.01	1.01
20	3005	38	1.26	1.27	1.28
21	4043	125	3.09	3.31	3.32
22	6545	76	1.16	1.25	1.25
23	3600	42	1.17	1.30	1.31
24	3992	43	1.08	1.20	1.20

Table B8: Results: 6 low PRF and 1 MPRF emitter, 166.67 MHz bandwidth

	Simulation Results			Predicted percentage	
emitter	pulses recvd	clashes	percentage	Poisson	Kazerman
19	6398	1011	15.80	13.34	14.18
20	3005	438	14.58	13.91	14.80
21	4043	833	20.60	19.27	20.76
22	6546	984	15.03	14.14	15.06
23	3601	554	15.38	14.03	14.93
24	3992	585	14.65	13.78	14.66
37	39995	3905	9.76	9.40	9.48

Table B9: Results: 6 low PRF and 1 HPRF emitters, 166.67 MHz bandwidth

	Simulation Results			Predicted percentage	
emitter	pulses recvd	clashes	percentage	Poisson	Kazerman
19	6400	2265	35.39	30.15	35.52
20	3005	1245	41.43	34.81	42.25
21	4043	4043	100.00	68.93	100.00
22	6548	3070	46.88	37.75	46.82
23	3601	1581	43.90	35.90	43.90
24	3992	1619	40.56	33.89	40.89
37	663995	14086	2.12	2.12	2.13

Table B10: Results: 6 low PRF and 2 MPRF emitters, 166.67 MHz bandwidth

	Simulation Results			Predicted percentage	
emitter	pulses recvd	clashes	percentage	Poisson	Kazerman
19	6398	2099	32.81	29.22	31.55
20	3005	972	32.35	30.12	32.57
21	4043	1730	42.79	38.65	42.52
22	6546	2168	33.12	30.59	33.13
23	3600	1188	33.00	30.31	32.80
24	3992	1288	32.26	29.92	32.35
37	39999	18199	45.50	39.01	45.30
38	60876	20103	33.02	30.14	33.01

Table B11: Results: 6 low PRF, 1 MPRF, 1 HPRF emitters, 166.67 MHz bandwidth

	Simulation Results			Predicted percentage	
emitter	pulses recvd	clashes	percentage	Poisson	Kazerman
19	6400	2880	45.00	38.85	44.10
20	3005	1507	50.15	43.15	50.16
21	4043	4043	100.00	74.06	100.00
22	6548	3541	54.08	45.88	54.26
23	3600	1869	51.92	44.16	51.64
24	3992	1935	48.47	42.31	48.94
37	40000	39999	100.00	92.23	100.00
38	663993	110211	16.60	15.59	16.61

Table B12: Results for 6 low PRF and 2 HPRF emitters, 166.67 MHz bandwidth

	Simulation Results			Predicted percentage	
emitter	pulses recvd	clashes	percentage	Poisson	Kazerman
19	6400	3288	51.38	45.43	51.45
20	3005	1775	59.07	51.66	59.52
21	4043	4043	100.00	86.90	100.00
22	6548	4218	64.42	55.49	64.66
23	3600	2212	61.44	53.08	61.41
24	3992	2294	57.46	50.46	57.95
37	520014	297155	57.14	44.26	57.31
38	664000	300486	45.25	37.09	45.39

Table B13: Results for first set of 6 low PRF emitters, 166.67 MHz bandwidth

	Simulation Results			Predicted percentage	
emitter	pulses recvd	clashes	percentage	Poisson	Kazerman
1	1389	8	0.58	0.70	0.70
2	2904	20	0.69	0.91	0.91
3	4420	37	0.84	0.75	0.75
4	2902	19	0.65	0.91	0.91
5	4480	26	0.58	0.75	0.75
6	9841	44	0.45	0.46	0.46

Table B14: Results for second set of 6 low PRF emitters, 166.67 MHz bandwidth

	Simulation Results			Predicted percentage	
emitter	pulses recvd	clashes	percentage	Poisson	Kazerman
7	3240	18	0.56	0.62	0.62
8	2902	15	0.52	0.57	0.57
9	2880	16	0.56	0.52	0.52
10	2609	18	0.69	0.65	0.65
11	2933	9	0.31	0.37	0.37
12	2883	18	0.62	0.61	0.61

Table B15: Results for third set of 6 low PRF emitters, 166.67 MHz bandwidth

	Simulation Results			Predicted percentage	
emitter	pulses recvd	clashes	percentage	Poisson	Kazerman
13	3120	21	0.67	0.60	0.60
14	2880	25	0.87	0.80	0.80
15	2000	15	0.75	0.87	0.87
16	5763	21	0.36	0.50	0.50
17	8464	45	0.53	0.40	0.40
18	3003	24	0.80	0.73	0.73

Table B16: Results for fifth set of 6 low PRF emitters, 166.67 MHz bandwidth

	Simulation Results			Predicted percentage	
emitter	pulses recvd	clashes	percentage	Poisson	Kazerman
25	5882	33	0.56	0.57	0.57
26	6733	24	0.36	0.58	0.58
27	3374	15	0.44	0.73	0.73
28	3237	15	0.46	0.84	0.84
29	3998	28	0.70	0.62	0.62
30	4042	15	0.37	0.47	0.47

Table B17: Results for sixth set of 6 low PRF emitters, 166.67 MHz bandwidth

	Simulation Results			Predicted percentage	
emitter	pulses recvd	clashes	percentage	Poisson	Kazerman
31	4402	29	0.66	0.70	0.70
32	3880	104	2.68	2.69	2.70
33	3311	45	1.36	1.32	1.32
34	6720	53	0.79	0.73	0.73
35	8138	52	0.64	0.66	0.66
36	9796	74	0.76	0.79	0.79

Table B18: Results for 1 low PRF and 1 MPRF emitter, 166.67 MHz bandwidth

	Simulation Results			Predicted percentage	
emitter	pulses recvd	clashes	percentage	Poisson	Kazerman
1	6398	799	12.49	12.45	13.30
2	39982	799	2.00	2.11	2.13

Table B19: Results for 1 low PRF and 1 HPRF emitter, 166.67 MHz bandwidth

	Simulation Results			Predicted percentage	
emitter	pulses recvd	clashes	percentage	Poisson	Kazerman
1	6400	2229	34.83	29.43	34.86
2	663991	2229	0.34	0.34	0.34

Table B20: Results for 2 low PRF emitters, 166.67 MHz bandwidth

	Simulation Results			Predicted percentage	
emitter	pulses recvd	clashes	percentage	Poisson	Kazerman
1	6384	5	0.08	0.08	0.08
2	2999	5	0.17	0.16	0.16

Table B21: Results for 2 low PRF and 1 MPRF emitters, 166.67 MHz bandwidth

	Simulation Results			Predicted percentage	
emitter	pulses recvd	clashes	percentage	Poisson	Kazerman
1	6399	804	12.56	12.52	13.37
2	3002	400	13.32	12.94	13.84
3	39982	1184	2.96	3.11	3.13

Table B22: Results for 2 low PRF and 1 HPRF emitters, 166.67 MHz bandwidth

	Simulation Results			Predicted percentage	
emitter	pulses recvd	clashes	percentage	Poisson	Kazerman
1	6400	2228	34.81	29.49	34.91
2	3003	1236	41.16	34.07	41.59
3	663992	3453	0.52	0.52	0.52

Table B23: Results for 3 low PRF emitters, 166.67 MHz bandwidth

	Simulation Results			Predicted percentage	
emitter	pulses recvd	clashes	percentage	Poisson	Kazerman
1	6390	41	0.64	0.61	0.61
2	2999	22	0.73	0.74	0.74
3	4040	53	1.31	1.28	1.28

Table B24: Results for 3 low PRF and 1 MPRF emitters, 166.67 MHz bandwidth

	Simulation Results			Predicted percentage	
emitter	pulses recvd	clashes	percentage	Poisson	Kazerman
1	6399	993	15.52	12.99	13.83
2	3001	463	15.43	13.45	14.34
3	4046	769	19.01	17.57	19.09
4	39983	2095	5.24	4.86	4.90

Table B25: Results for 3 low PRF and one HPRF emitters, 166.67 MHz bandwidth

	Simulation Results			Predicted percentage	
emitter	pulses recvd	clashes	percentage	Poisson	Kazerman
1	6400	2243	35.05	29.87	35.26
2	3003	1258	41.89	34.45	41.93
3	4046	4045	99.98	68.28	100.00
4	663990	8026	1.21	1.21	1.21

Table B26: Results for 4 low PRF emitters, 166.67 MHz bandwidth

	Simulation Results			Predicted percentage	
emitter	pulses recvd	clashes	percentage	Poisson	Kazerman
1	6395	54	0.84	0.82	0.82
2	3000	31	1.03	1.01	1.01
3	4040	92	2.28	2.25	2.25
4	6540	62	0.95	0.94	0.94

Table B27: Results for 4 low PRF and 1 MPRF emitters, 166.67 MHz bandwidth

	Simulation Results			Predicted percentage	
emitter	pulses recvd	clashes	percentage	Poisson	Kazerman
1	6399	849	13.27	13.17	14.01
2	3002	459	15.29	13.68	14.57
3	4044	803	19.86	18.38	19.89
4	6543	970	14.83	13.86	14.79
5	39987	2798	7.00	7.01	7.08

Table B28: Results for 4 low PRF and 1 HPRF emitters, 166.67 MHz bandwidth

	Simulation Results			Predicted percentage	
emitter	pulses recvd	clashes	percentage	Poisson	Kazerman
1	6400	2257	35.27	30.01	35.40
2	3003	1289	42.92	34.63	42.09
3	4046	4046	100.00	68.59	100.00
4	6546	3052	46.62	37.55	46.65
5	663996	11025	1.66	1.66	1.66

Table B29: Results for 5 low PRF emitters, 166.67 MHz bandwidth

	Simulation Results			Predicted percentage	
emitter	pulses recvd	clashes	percentage	Poisson	Kazerman
1	6395	62	0.97	0.92	0.92
2	3000	32	1.07	1.14	1.15
3	4040	124	3.07	2.76	2.77
4	6540	76	1.16	1.09	1.10
5	3600	56	1.56	1.16	1.17

Table B30: Results for 5 low PRF and 1 MPRF emitters, 166.67 MHz bandwidth

	Simulation Results			Predicted percentage	
emitter	pulses recvd	clashes	percentage	Poisson	Kazerman
1	6398	854	13.35	13.26	14.10
2	3003	441	14.69	13.80	14.69
3	4044	829	20.50	18.81	20.31
4	6544	972	14.85	14.00	14.92
5	3600	530	14.72	13.90	14.81
6	39986	3235	8.09	8.16	8.23

Table B31: Results for 5 low PRF and 1 HPRF emitters, 166.67 MHz bandwidth

	Simulation Results			Predicted percentage	
emitter	pulses recvd	clashes	percentage	Poisson	Kazerman
1	6400	2258	35.28	30.08	35.46
2	3003	1267	42.19	34.72	42.17
3	4046	4045	99.98	68.76	100.00
4	6546	3034	46.35	37.65	46.74
5	3600	1560	43.33	35.81	43.82
6	663991	12510	1.88	1.89	1.89

Modelling Time-of-Arrival Ambiguities in a Combined Acousto-optic and Crystal Video Receiver

Simon Rockliff

	Number of Copies
DGFD(Air)	1
Defence Science and Technology Organisation	
Chief Defence Scientist; FAS Science Policy AS Science Corporate Management	1
Counsellor, Defence Science, London	Doc Cntl Sht
Counsellor, Defence Science, Washington	Doc Cntl Sht
Senior Defence Scientific Adviser/Scientific Adviser, POLCOM	1
Director, AMRL	1
Navy Scientific Adviser	1
Air Force Scientific Adviser	1
Scientific Adviser, Army	1
Director Trials	1
Electronics and Surveillance Research Laboratory	
Chief, Electronics Warfare Division	1
Research Leader Signal and Information Processing	1
Head, Electronic Support Measures Systems	1
Head, Information and Signal Processing	1
Mr. M. Brown, ISP group	1
Dr. S Kelly, ESMS group	1
Mr. W. Adderley, ISP group	1
Dr. S. Rockliff, ESMS group	1
DSTO Library	
DSTO Library Salisbury	2
DSTO Library Maribynong	1
DSTO Library Fishermens Bend	1
DSTO Library Pyrmont	Doc Cntl Sht
Defence Central	
OIC TRS, Defence Central Library, Technical Reports Centre	1

OIC Document Exchange Centre (for retention)	1
United States Defense Technical Information Center	2
United Kingdom Defence Research Information Centre	2
Canada Defence Scientific Information Service	1
New Zealand Defence Information Centre	1
Library, Defence Intelligence Organisation	1
Library, Defence Signals Directorate	Doc Cntl Sht
Army	
Director General Force Development (Land)	Doc Cntl Sht
Air Force	
OIC ATF ATS, RAAFSTT, WAGGA	2
Navy	
Director General Force Development (Sea)	Doc Cntl Sht
Spares	
DSTO Library Salisbury	6

Department of Defence

DOCUMENT CONTROL DATA SHEET

1. Page Classification	
UNCLASSIFIED	
2. Privacy Marking/Caveat	

3a. AR Number	3b. Establishment Number	3c. Type of Report	4. Task Number
AR-009-439	DSTO-RR-0062	RESEARCH REPORT	AIR-92/194

5. Document Date	6. Cost Code	7. Security Classification	8. No. of Pages	40
NOVEMBER 1995	819920	[L] Document [U] Title [U] Abstract	9. No. of Refs	8

10. Title
MODELLING TIME-OF-ARRIVAL AMBIGUITIES IN A COMBINED ACOUSTO-OPTIC AND CRYSTAL VIDEO RECEIVER

S (Secret C (Confi) R (Rest) U (Unclass)

* For UNCLASSIFIED docs with a secondary distribution LIMITATION, use (L) in document box.

11. Author(s)
SIMON ROCKLIFF

12. Downgrading/ Delimiting Instructions
Limitation to be reviewed in October 1998

13a. Corporate Author and Address
Electronic Warfare Division
Electronics and Surveillance Research Laboratory
PO Box 1500 SALISBURY SA 5108

13b. Task Sponsor
DGFD(Air)

14. Officer/Position responsible for

Security	SOESRL
Downgrading	CEWD
Approval for release	CEWD

15. Secondary Release Statement of this Document

Access additional to the initial distribution list is limited to the Defence Organisations of Australia, US, UK, Canada and New Zealand. Others MUST be referred to Chief, Electronic Warfare Division, ESRL.

Any enquiries outside stated limitations should be referred through DSTIC, Defence Information Services, Department of Defence, Anzac Park West, Canberra, ACT 2600.

16a. Deliberate Announcement

May be announced to the Defence Organisations of Australia, UK, US, Canada and New Zealand.

16b. Casual Announcement (for citation in other documents)

[√] No Limitation [ ] Ref. by Author, Doc No and date only

17. DEFTEST Descriptors: Radiofrequency interference, Crystal video receivers, Acousto optical devices

18. DISCAT Subject Codes

19. Abstract

The probability of pulses overlapping in time being received by a combined acousto-optic/crystal video receiver is investigated. Theoretical analysis and computer simulation results are compared for a variety of high pulse density scenarios and for two crystal video band configurations. Upper and lower bounds are derived for the probability of coincidence. It is shown that a small number of high duty cycle emitters will cause an unacceptable number of pulses in that bandwidth. The number of frequency subbands with crystal detectors required to cover the acousto-optic receiver bandwidth is therefore a compromise between cost and complexity of implementation.

DEPARTMENT OF DEFENCE
DEFENCE SCIENCE & TECHNOLOGY ORGANISATION
DSTO

SCIENCE CORPORATE MANAGEMENT BRANCH
DSTO SALISBURY LIBRARY-REPORTS DISTRIBUTION
PO BOX 1500 SALISBURY SA 5108

Reference: R9607/7/9
Contact: Natalie Mahlknecht
E-mail: natalie.mahlknecht@dsto.defence.gov.au

Telephone: (08) 8259 6255
Facsimile: (08) 8259 6803

27th August 1999

AD-B208 950

To All Copyholders
cc: To the Team Leader of Records & Archives

Notification of Downgrading/ Delimiting of DSTO Report

Please note that the Release Authority has authorised the downgrading/ delimiting of the report detailed here:

DSTO NUMBER	**DSTO-RR-0062**
AR NUMBER	**AR-009-439**
FILE NUMBER	**UNKNOWN**
REVISED CLASSIFICATION / RELEASE LIMITATION	**UNCLASSIFIED** **No Limitations** Approved for Public Release

Please amend your records and make changes to your copy of the report itself to reflect the new classification/ release limitation.

Natalie Mahlknecht
Reports Distribution
DSTO Library, Salisbury

Received 6-5-2000